Materials Research, Vol. 5, No. 2, 165-172, 2002.

Characterization of Sintered and Sintered/Plasma-Nitrided Fe-1.5% Mo Alloy by SEM, X-Ray Diffraction and Electrochemical Techniques

José de Pinho Alves Neto[a], Cristiano Giacomelli[a], Aloísio Nelmo Klein[b], Joel Louis Rene Muzart[b], Almir Spinelli[a]*

[a] *GEPEEA - Grupo de Estudos de Processos Eletroquímicos e Eletroanalíticos, Departamento de Química, Centro de Ciências Físicas e Matemáticas, Universidade Federal de Santa Catarina, 88040-900 Florianópolis - SC, Brazil*

[b] *LABMAT - Laboratório Interdisciplinar de Materiais, Departamento de Engenharia Mecânica, Centro Tecnológico, Universidade Federal de Santa Catarina, 88040-900 Florianópolis - SC, Brazil*

Received: October 5, 2001; Revised: April 2, 2002

Electrochemical experiments together with SEM and X-Ray techniques were carried out in order to evaluate the corrosion resistance, to analyze the surface condition and to characterize the nitride layer of the sintered and sintered/plasma-nitrided Fe-1.5% Mo alloy in $Mg(NO_3)_2$ 0.5 mol.L^{-1} solution (pH 7.0). The sintered/plasma-nitrided samples presented a higher corrosion resistance, indicating that the surface treatment improved the electrochemical properties of the sintered material. In addition, the nitride layer formed at 500 °C showed better corrosion resistance that the layers formed at higher temperatures. This difference can be ascribed to the nitrogen content in the nitride layer, which at 500 °C is higher due to the formation of a phase rich in nitrogen (ε phase) while at higher temperatures a phase poor in nitrogen (γ' phase) is formed.

Keywords: *Fe-Mo alloy, powder metallurgy, plasma-nitriding, corrosion*

1. Introduction

It is well known that the production costs of sintered steels are significantly lower than those of steels produced by the conventional methods involving foundry, shape and finish procedures, principally in serial production of pieces with narrow dimensional tolerances. However, materials obtained via powder metallurgy have low corrosion resistance due, fundamentally, to the presence of residual pores. To increase the corrosion resistance of sintered materials, simple methods as immersion in oil and painting or coating[1-2] have been proposed. More elaborated protection methods as steam treatment[3-4] and dacronizing[5] are also sometimes recommended. In addition, plasma-nitriding techniques[6-10] are being used with success for superficial treatment aiming to improve the mechanical properties[11-15] and the corrosion resistance of stainless steels[16-20] and low alloy steels[21-27] manufactured through powder metallurgy.

In the plasma-nitriding process, factors such as cleaning of the sample, composition and flow rate of N_2/H_2 mixture, treatment time and temperature determine the properties of the formed nitride layer[6-10] and, consequently, they have significant influence upon the corrosion resistance.

In this work was carried out the study of the corrosion resistance of sintered steel containing 1.5% Mo and nitrided at different temperatures. The Mo was chosen because it stabilizes the ferrite, responds very well to the thermo-chemical treatments involved in the formation of superficial layers and improves the corrosion resistance of ferrous materials[26-27].

2. Material and Methods

2.1. Sintering

The preparation of the samples was done according to the conventional powder metallurgy pathway, consisting of mixture, compacting and sintering steps under a protective atmosphere. The binary sintered Fe-1.5% Mo alloy was obtained using a mixture of 97.7% Fe, 1.5% Mo powders and 0.8% zinc stearate. The sintering conditions were as follows: compacting at 600 MPa; dewaxing for 30 minutes

*e-mail: spin@qmc.ufsc.br

at 550 °C under H_2 flux; time: 120 minutes; temperature: 1250 °C; atmosphere: ultra-pure H_2. After sintering the samples were cleaned with petroleum ether to remove grease, oil and others residues. In critical cases, the samples were cleaned in an ultra-sonic bath for 10 minutes.

2.2. Nitriding

Before accomplishing the nitriding process the samples were cleaned in the reactor. The cleaning conditions were: H_2 flux: 2 $cm^3.s^{-1}$; pressure: 134 Pa; time: 15 minutes; voltage: 400 V. The nitriding process conditions were: gas mixture composition: 20% H_2/80% N_2; total flux of gas: 2 $cm^3.s^{-1}$; pressure: 400 Pa; time of nitriding: 120 minutes (after attaining the suitable temperature); voltage: 380-500 V. The nitriding temperature was the only variable parameter in this treatment. The objective of varying the temperature was to obtain nitride layers with different compositions[11]. At 500 °C the ε phase is preferentially formed and at 580 °C the γ'phase is predominant. The investigated temperatures were 500, 540, 560 and 580 °C. After nitriding process the samples were cooled down in H_2 flux to 30 °C.

2.3. Electrochemical measurements

The electrochemical measurements were performed with the EG&G-PARC model 263A system coupled to a personal computer. Data gathering was controlled by the EG&G-PARC "SoftCorr Corrosion Measurement Software Model 252/352". $Mg(NO_3)_2$ 0.5 $mol.L^{-1}$ solution was used as testing electrolyte. The pH of this solution, measured with an Orion model 720A pHmeter, was adjusted to 7.0 by adding 0.01 mol. L^{-1} NaOH. The solutions were prepared with water obtained by treatment in a Millipore Mille-Q system and p.a. reagents. The electrochemical tests were performed in non-deaerated solutions at laboratory room temperature. A conventional three electrodes cell was employed to electrochemical tests. The working electrodes (sintered and sintered/plasma-nitrided Fe-1.5% Mo samples) were not submitted to any superficial treatment (electrochemical or mechanical polish) before each experiment. Two graphite rods were used as auxiliary electrodes and a saturated calomel electrode (SCE) was used as reference, but all potentials mentioned are referred to the standard hydrogen electrode (SHE) scale. The determination of corrosion potential (E_{corr}) x time curves and of potentiodynamic polarization curves was performed according to the ASTM G5 standard practice. The corrosion potential value was followed during 60 minutes. Soon after, it was applied to the working electrode, for 2 min, a cathodic potential (-400 mVxE_{corr}), in order to reduce the eventual oxides formed during the E_{corr} measurements. The following step consisted in obtaining the potentiodynamic polarization curve, starting from the potential -250 mV *vs.* E_{corr} up to 1.6 V/SHE. The scan rate was always of 0.8 $mV.s^{-1}$. The corrosion parameters E_{corr}, R_p, E(I=0), i_{corr} and corrosion rate were obtained considering the geometrical area of the working electrode (0.28 cm^2). As for the sintered material the real area is much higher, the values of corrosion parameters should be seen as comparative and not absolute values. The experimental errors do not exceed 10%.

2.4. Samples characterization

In order to characterize the samples and the layers formed by nitriding surface treatment, the following methods were used together with the electrochemical measurements: surface analysis by scanning electronic microscopy-SEM (Philips XL 30) and structure analysis of the nitride layers by X-Ray diffraction (Philips X'PERT).

3. Results and Discussions

3.1. Sintered samples

Characterization by SEM

The samples of sintered Fe-1.5% Mo presented on average a density of 7.0 $g.cm^{-3}$, a value lower than the theoretical value of 7.8 $g.cm^{-3}$. This difference indicates the presence of pores in the samples. These pores are inherent to the used manufacturing process: uniaxial matrix of double effect and sintering in a tubular oven.

Figure 1A is the micrograph of the sintered sample cross section, showing the presence of pores. Two different types of pores are distinguishable: round pores, also know as secondary pores, which are formed during the sintering process; and irregular pores, which are formed during the compacting process. Fig. 1B is the micrograph of the sintered sample surface, which also shows the presence of pores. Fig. 1B can be used as reference to show the effect of the surface treatments and the surface condition of the samples before the corrosion tests.

3.2. Sintered/plasma-nitrided samples

Characterization by X-Ray diffraction

Figure 2 shows the X-ray diffraction spectra of the sintered samples nitrided at different temperatures. In Fig. 2A is observed that the main nitride layer formed at 500 °C is the ε layer. As the temperature increases (Figures 2B-2D) the γ' layer becomes preponderant, indicating a decrease in the nitrogen layer concentration. These results are in agreement with the previous results published by Fontana[11] and confirm that the nitriding temperature has influence on the composition of the formed nitride layer.

3.3. Corrosion tests

Reproducibility of the experiments

In corrosion studies, the reproducibility of experiments is very important to warrant the results credibility. The reproducibility of the corrosion experiments is still more difficult

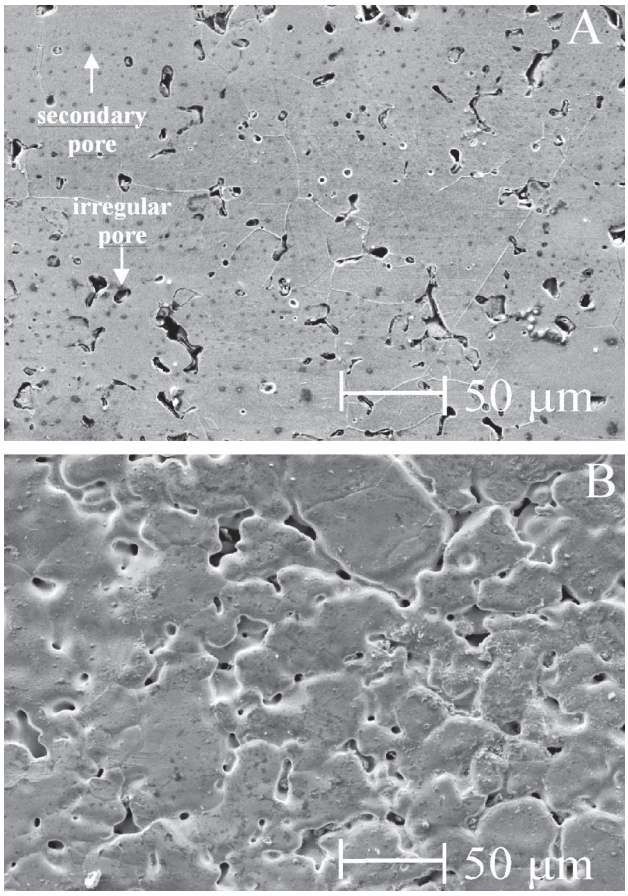

Figure 1. Micrograph of sintered Fe-1.5% Mo samples. (A) cross section, (B) surface view ($t_{sintering}$ 2.0 h; $T_{sintering}$ 1250 °C).

when sintered steels are studied, because it is practically impossible to prepare samples with identical surfaces. However, if the steps of sintering, nitriding and cleaning of the samples are carefully controlled, reproducible electrochemical results can be obtained, as show in the Fig. 3. The Figs. 3A and 3B show the E_{corr} x time curves for sintered and sintered/plasma-nitrided samples, respectively. For each material three experiments were carried out with different samples. It can be observed the high reproducibility of the experiments. The Figs. 3C and 3D show the potentiodynamic polarization curves for the same samples used in the E_{corr} x time experiments. In these cases also a very good reproducibility was obtained. The results shown in Figs. 3A-3D demonstrate that very reproducible data can be obtained from electrochemical experiments with sintered and sintered/plasma-nitrided samples if the steps of preparation and cleaning of the samples are cautiously controlled.

Ecorr x time curves

Figure 4 shows the E_{corr} x time curves for the sintered, sintered/plasma-nitrided at 500 °C (Fig. 4A) and sintered/

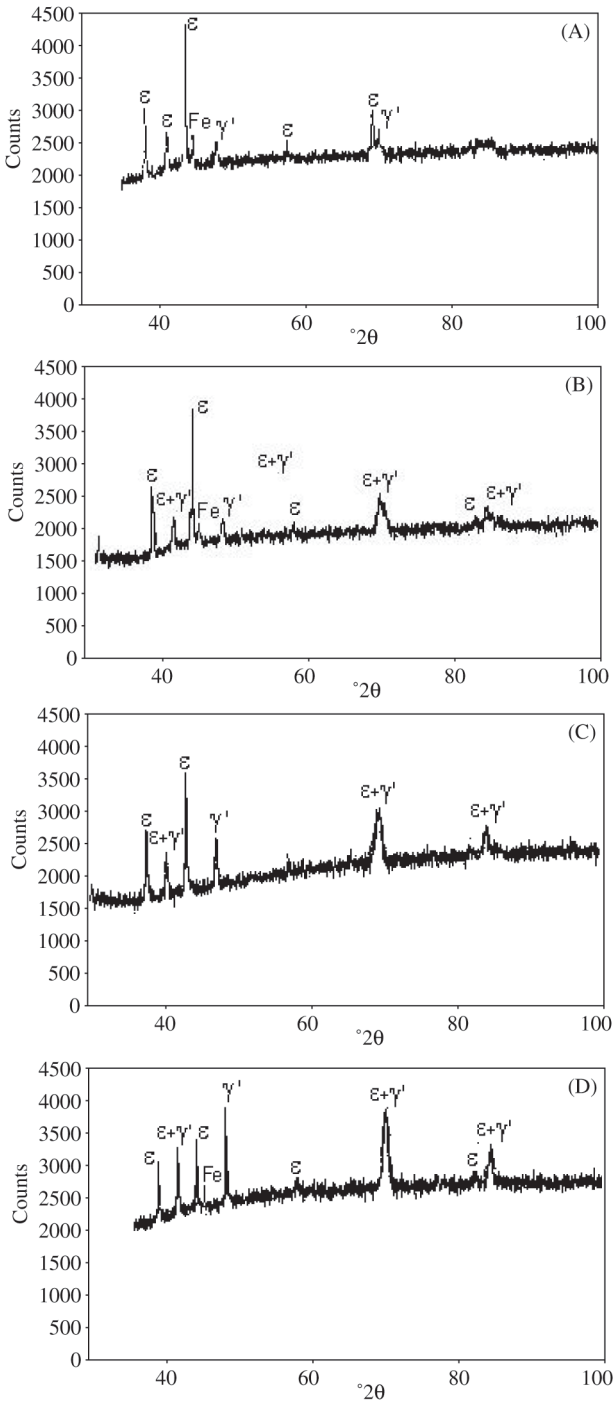

Figure 2. X-Ray diffraction spectra for the sintered/plasma-nitrided Fe-1.5% Mo samples. Nitriding temperatures (A) 500 °C (B) 540 °C, (C) 560 °C, (D) 580 °C.

plasma-nitrided at different temperatures (Fig. 4B) Fe-1.5% Mo alloy. It can be observed that at the beginning of each experiment a high E_{corr} is measured, which decays quickly. The initial high potential is probably due to the oxide film

formed, since the samples were exposed to the atmosphere and they can be experienced a certain degree of oxidation. After immersion this films undergoes reductive dissolution and the corrosion potential decreases. It is also possible that adsorbed particles remainder of the samples elaboration cover the surface. In contact with the testing electrolyte these particles are desorbed leaving the surface exposed to the solution. Consequently an active dissolution process is initiated and the E_{corr} decreases rapidly. After 10-20 minutes the E_{corr} stabilizes for practically all samples. Comparing the sintered and the sintered/plasma-nitrided samples (Fig. 4A) it is observed that for the plasma nitrided sample the E_{corr} is nobler, indicating that the nitriding process promoted a significant anodic reaction rate inhibition. For the

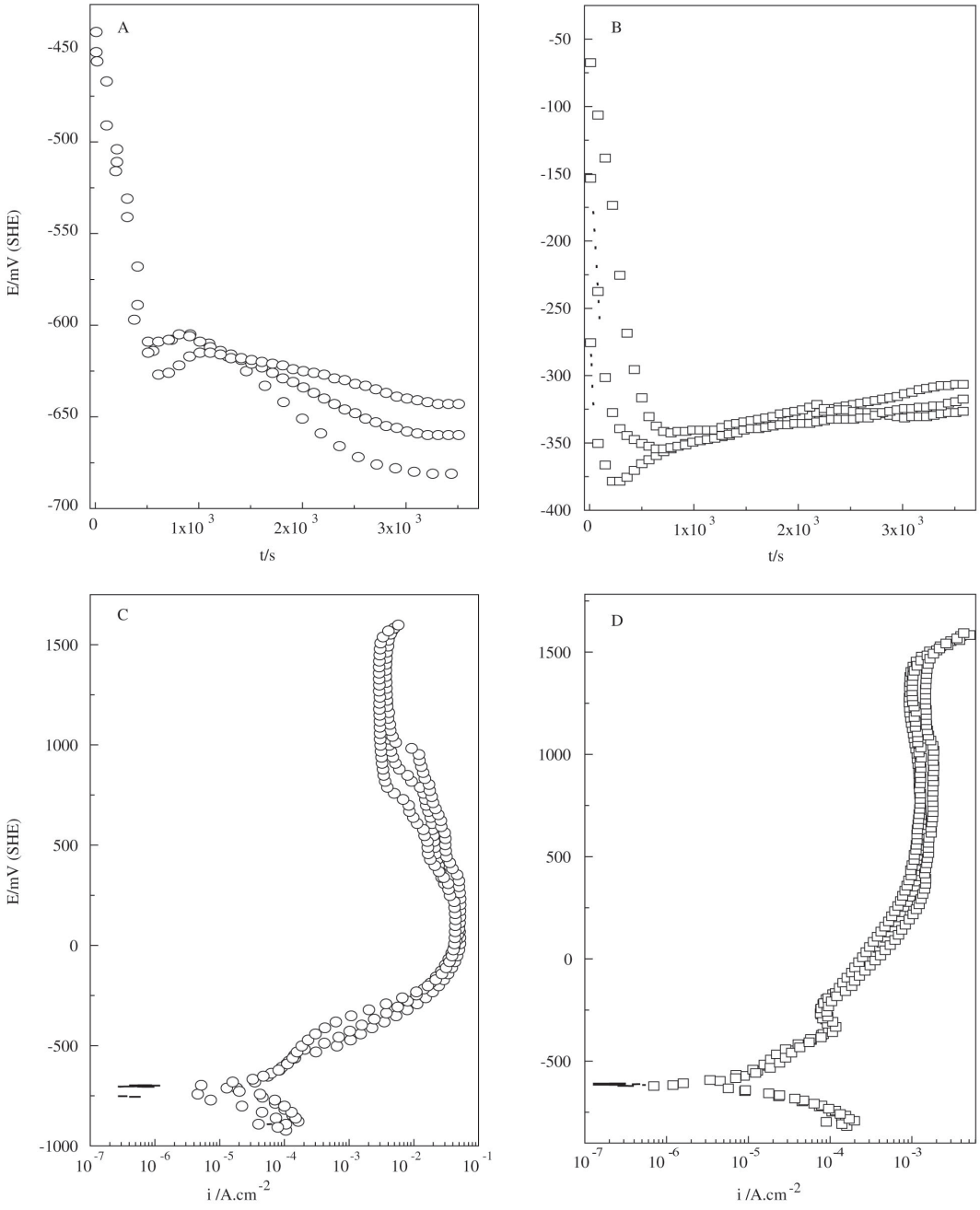

Figure 3. Reproducibility of the E_{corr} x time curves and potentiodynamic polarization curves for the (A, C, respectively) sintered and (B, D, respectively) sintered/plasma-nitrided Fe-1.5% Mo alloy.

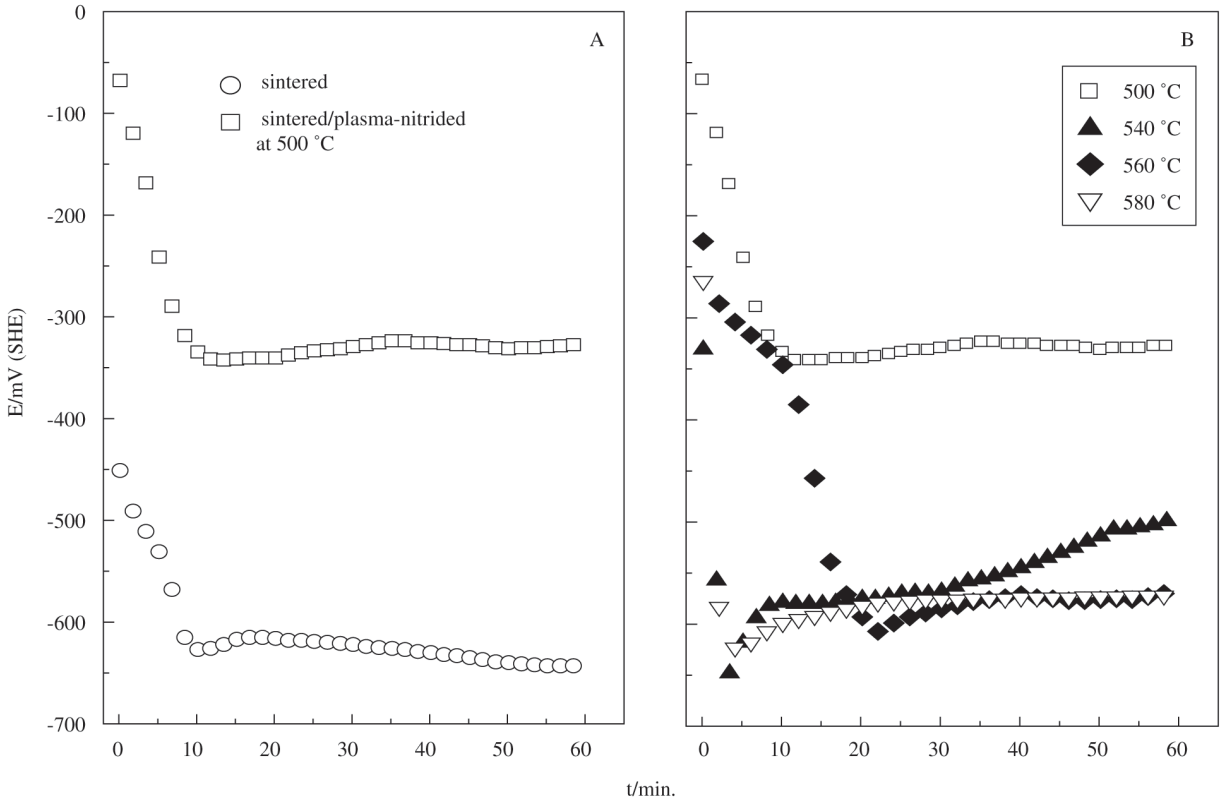

Figure 4. E_{corr} x time curves in 0.5 mol.L^{-1} $Mg(NO_3)_2$ solution (pH 7.0) for the sintered and sintered/plasma-nitrided Fe-1.5% Mo samples. (A) Sintered and sintered/plasma-nitrided at 500 °C, (B) sintered/plasma-nitrided at different temperatures.

sintered/plasma-nitrided at different temperature samples (Fig. 4B) it is observed that as the nitriding temperature decreases the E_{corr} stabilizes at less negative potentials. It is observed that the E_{corr} of the sample nitrided at 500 °C stabilizes at a less negative potential than the others, indicating that the nitriding process at this temperature renders a nobler character to the sintered Fe-1.5% Mo alloy. The differences observed in Fig. 4B can be related with the composition of the nitride layer, in agreement with the results obtained by X-Ray diffraction. In this sense, we can suppose that the nitride layer formed at 500 °C (ε phase) confers a higher corrosion resistance to the sintered sample that the nitride layer formed at higher temperatures (γ' phase).

Potentiodynamic polarization curves

Figure 5 shows the potentiodynamic polarization curves for the sintered and sintered/plasma-nitrided at 500 °C (Fig 5A) and sintered/plasma-nitrided at different temperatures (Fig. 5B) Fe-1.5% Mo alloy. In the Figure 5A can be observed that for the sintered sample the anodic dissolution region is very large and passivation occurs only in potentials superior at above +100 mV/SHE. In addition, deposits of corrosion products were observed at the bottom of the electrochemical cell at the end of the experiments, due to the large dissolution process. For the sintered/plasma-nitrided at 500 °C sample the current densities are lower, the anodic dissolution region is small and a passivation potential is observed at -80 mV/SHE. After the anodic peak the current density increases, reaching values similar to those of the sintered sample around 1000 mV/SHE. However, for the sintered/plasma-nitrided sample, no corrosion products were observed at the end of the experiments. The position of the anodic peak depends on the nitriding temperature (Fig. 5B). For temperatures of 540 and 560 °C the anodic peak is observed at around -250 mV/SHE. For 580 °C the anodic peak is not clearly observed. By comparing the potentiodynamic polarization curves it is verified that the current density for the sintered/plasma-nitrided samples (for all temperatures) is lower than the current density for the sintered samples, at any potential. This feature suggests that the nitriding process confers a higher corrosion resistance to the sintered Fe-1.5% Mo alloy.

In the Table 1 are presented the corrosion parameters obtained from the potentiodynamic polarization curves.

Comparing the polarization resistance (R_p) values for the sintered and the sintered/plasma-nitrided at 500 °C sam-

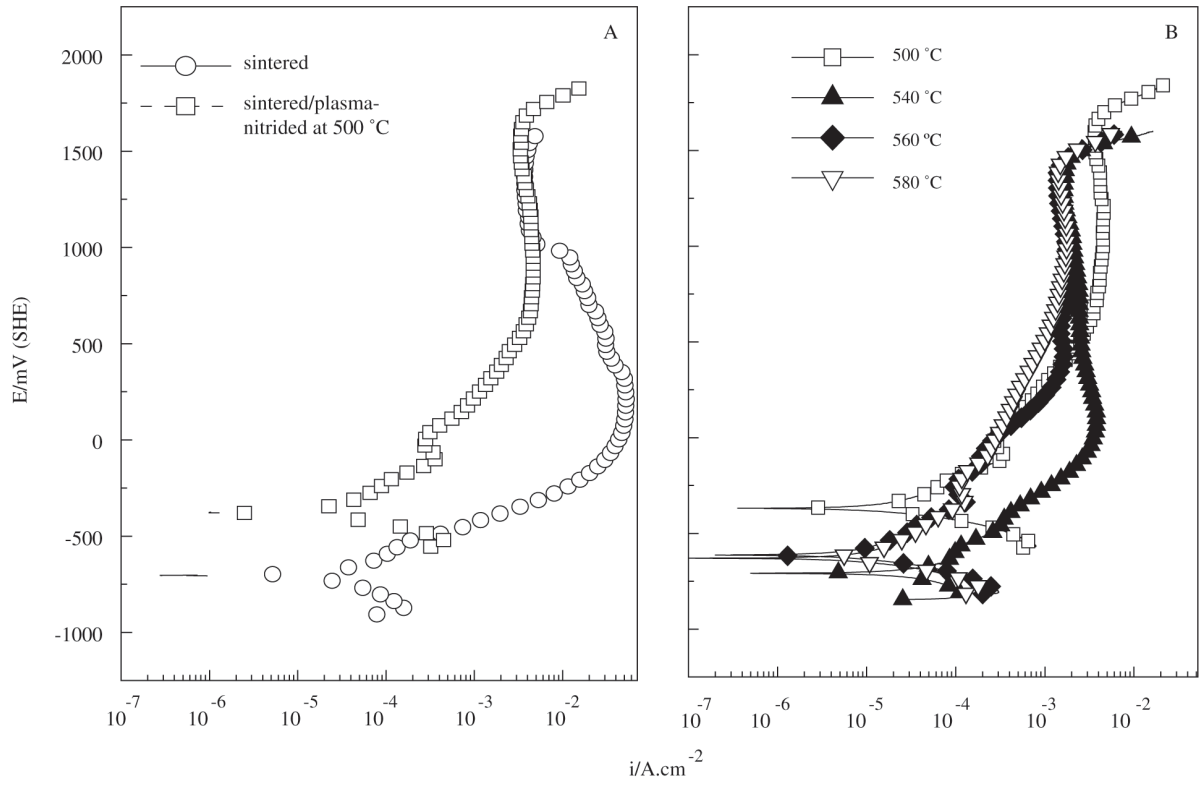

Figure 5. Potentiodynamic polarization curves in 0.5 mol.L^{-1} $Mg(NO_3)_2$ solution (pH 7.0) for the sintered and sintered/plasma-nitrided Fe-1.5% Mo samples. (A) Sintered and sintered/plasma-nitrided at 500 °C, (B) sintered/plasma-nitrided at different temperatures.

Table 1. Corrosion parameters for sintered and sintered/plasma-nitrided Fe-1.5% Mo alloy.

Sample	Sintered	Sintered/plasma-nitrided			
Temperature		500 °C	540 °C	560 °C	580 °C
R_p (kohm.cm^2)	3.71	16.89	12.56	10.35	7.10
i_{corr} (μA.cm^{-2})	265.0	60.40	68.45	95.35	107.5
E (mV) (I=0)	-600.0	-317.5	-343.9	-419.0	-572.0
Corrosion rate (mm/year)	0.939	0.300	0.356	0.388	0.566

ples a value 5 times greater is observed for the nitrided sample, indicating that the nitride layer increases its corrosion resistance. As expected, the corrosion current density (i_{corr}) is also lower for the sample submitted to the surface treatment. Moreover, the potential where the current is zero E(I=0) for the sintered sample is more negative than the E(I=0) for the sintered/plasma-nitrided at 500 °C sample, indicating a nobler character of the alloy covered by nitride layer. The corrosion rates values also indicate a better performance of the sintered/plasma-nitrided sample in terms of corrosion resistance. The parameters above, in particular the corrosion rate values, were obtained considering the geometrical area of the working electrodes. They cannot be seen as absolute values, because the real area was not determined. They were calculated for to permit the comparison between samples submitted and not submitted to the surface treatment.

The R_p values for the sintered/plasma-nitrided at different temperatures samples decrease as the nitriding temperature increases. It is observed, however, that the lowest value found for the sintered/plasma-nitrided samples is still larger than the value found for the sintered sample. Analyzing the values of the corrosion current density, an increase is verified as the nitriding temperature increases, in agreement with the R_p values. For the E(I=0) values, a decrease is observed as the nitriding temperature increases, indicating a character less noble for the sample nitrided at 580 °C and a character more noble for the sample nitrided at 500 °C. Even if a small difference between the values is observed, the corrosion rate for the nitrided at 500 °C sample is the smallest

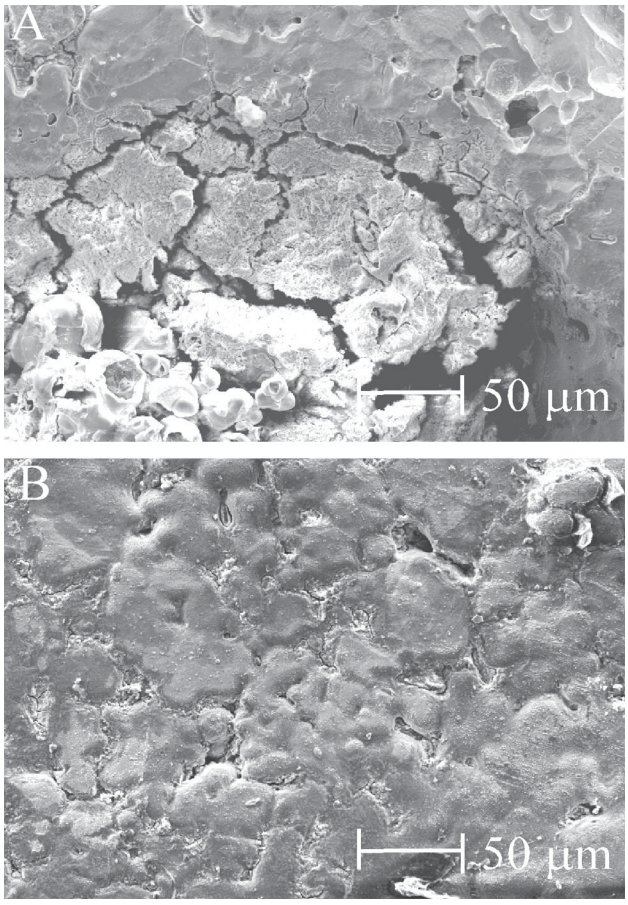

Figure 6. Micrographs of (A) sintered and (B) sintered/plasma-nitrided at 500 °C Fe-1.5% Mo samples after corrosion tests.

one. This result demonstrates that the sample nitrided at 500 °C, in which there is a predominance of the ε phase in the nitrided layer (Fig. 1A), is more corrosion resistant. The sample nitrided at 580 °C, in which the γ' phase prevails in the nitrided layer (Fig. 1D), is less corrosion resistant. The main difference between the ε and the γ' phases in the nitride layers is the nitrogen content. In the former the nitrogen content is higher. Therefore, we can conclude that the nitrogen concentration in the nitrided layer is a decisive factor for corrosion resistance.

Comparing the E_{corr} values in the Fig. 1 and the E(I=0) values shows in Table 1, a good concordance is observed. These corrosion parameters obtained from different techniques are coherent with the other corrosion parameters obtained for the samples submitted and not submitted to the surface treatment.

Surface analysis by SEM technique after the corrosion tests

Figure 6 shows the micrographs for the sintered and sintered/plasma-nitrided Fe-1.5% Mo samples after the corrosion tests. The micrograph of the sintered sample (Fig. 6A) shows that the corroded surface was practically destroyed. The white areas are due to the deposited $Mg(NO_3)_2$, demonstrating the occurrence of an intense corrosion process. The micrograph of Fig. 6B shows the surface of a sintered/plasma-nitrided at 500 °C sample after the corrosion tests. It can be observed that this surface remained practically intact, with the pores closed. Comparing the Figs. 6A and 6B, we can verify that the surface of sintered sample was more attacked than the surface of nitrided sample. Therefore, it is clear that the nitride layer increases the corrosion resistance of the sintered material.

The micrographs of samples nitrided at other temperatures showed the same aspect of the sample nitrided at 500 °C. In all cases the surfaces remained practically intact, what suggests that, independently of the nitriding temperature, the nitride layer increases the corrosion resistance.

The surface analysis confirmed the results obtained in corrosion tests. The nitride layer, in particular the one obtained at 500 °C, grants a nobler character to the samples, providing a better performance in terms of corrosion when compared with the sintered samples.

4. Conclusions

The plasma-nitriding process showed to be viable in the treatment of the porous surfaces, as is the case of the sintered Fe-1.5% Mo alloy. Without exception, all the sintered/plasma-nitrided samples presented a higher corrosion resistance than the sintered samples. The influence of the nitrogen concentration in the nitrided layer was also evidenced by the corrosion experiments. In the nitride layers obtained at 500 °C prevails the ε phase rich in nitrogen which grants a better electrochemical stability to the sintered alloy than the γ' phase, which is formed at temperatures higher than 540 °C and is poor in nitrogen. The micrographs obtained by SEM technique for the samples after the corrosion experiments were in accord with the electrochemical results. The samples with higher corrosion rate showed the surface visibly more corroded. We can conclude that the nitride inorganic coating grants a better electrochemical stability to the sintered Fe-1.5% Mo binary alloy.

Acknowledgements

The authors thank to CNPq for financial support.

References

1. Klar E.; Samal P.K. *Powder Metals in Corrosion Tests and Standards: Application and Interpretation*, Robert Baboian editor, ASTM Manual series: MNL 20, USA, 1995.
2. Metals Handbook, *Powder Metallurgy*, Klar E. Coordi-

nator, ASM, Metals Park, Ninth Edition, OH, v. 7, 1984.
3. Orzeske, D.J. *Industrial Heat Treating*, v. 63, p. 34, 1986.
4. Feinberg, D. *Surface Finishing of Powder Metallurgy Parts*, Metal Powder Industries Federation, Princeton, NJ, 1968.
5. Hanada, M.; Amano, N.; Takeda, Y. *et al. International Congress and Exposition*, SAE Technical Paper Series 890407, Detrit, MI, 1989.
6. Chapman, B. *Glow Discharge Process*, John Wiley & Sons, Inc. NY, 1980.
7. Hudis, M. *Journal of Applied Physics*, v. 44, p. 1489, 1983.
8. Wried, H.A.; Zwell, L. Trans AIME, p. 1242, 1962 (in Leslie, W. C. *The Physical Metallurgy of Steels*, McGraw-Hill Book Company, 1981).
9. Juza, R. *Advances in Inorganic Chemistry*, H.J. Emeléus, v. 9, p. 81, 1966.
10. Jack, K.H. *Acta Crystographica*, v. 5, p. 404, 1952.
11. Fontana, L.C. Masters Thesis, Universidade Federal de Santa Catarina, Florianópolis, Brazil, 1991.
12. Maliska, A.M. Thesis, Universidade Federal de Santa Catarina, Florianópolis, Brazil, 1995.
13. Kühn-Arroyo, I.; Maliska, A.M.; Chimello Jr. O., Cattoni V., *Anais do 11° CBECIMAT*, Águas de São Pedro, SP, Brazil, p. 63, 1994.
14. Maliska, A.M.; Klein A.N.; Souza, A.R. *ABM - IV Seminário de Metalurgia do Pó*, São Paulo, SP, p. 389, 1995.
15. Borges, P.C.; Bonsiep, S.T.G.; Klein, A.N.; Snoijer, B. *Anais do 11° CBECIMAT*, Águas de São Pedro, SP, p. 51, 1994.
16. Becker, B.S.; Bolton J.D.; Eagles, A.M. *P. I. Mech. Eng. L – J. Mat.*, v. 214, p. 139, 2000.
17. Baran, M.C.; Shaw, B.A. *Int. J. Powder Metall.*, v. 36, p. 57, 2000.
18. Otero, E.; Pardo, A.; Utrilla, V.; Sáenz, E.; Álvarez, J.F. *Corros. Sci.*, v. 40, p. 1421, 1998.
19. Otero, E.; Pardo, A.; Utrilla, V.; Pérez, F. J.; Merino, C. *Corros. Sci.*, v. 39, p. 453, 1997.
20. Nazmy, M.Y.; Karner, W.; Algwaiz, A.A. *J. Metals*, v. 30, p. 14, 1978.
21. Pereira, N.C.; Mittelstädt, F.G.; Spinelli, A.; Maliska, A.M.; Klein, A.N.; Muzart, J.L.R.; Franco, C.V. *Journal of Materials Science*, v. 30, p. 4817-4822, 1995.
22. Debata, M., Upadhyaya, G.S., *Indian J. Eng. Mater. S.*, v. 8, p. 153, 2001.
23. Sobral, A.V.C.; Parente, A.C.B.; Muzart, J.L.R.; Franco, C.V. *Surf. Coat. Technol.*, v. 92, p. 10, 1997.
24. Kushchevskaya, N.F. *Powder Metallurgy and Metal Ceramics*, v. 35, p. 211, 1996.
25. Maliska, A.M.; Klein, A.N.; De Souza, A.R. *Surf. Coat. Technol.*, v. 70, p. 175, 1995.
26. Danninger, H.; Kara, T. *Powder Metall. Int.*, v. 20, p. 9, 1988.
27. Spalvins, T. *J. Vac. Sci. Technol.*, v. A3, p. 2329, 1985.